Investigation of 5G Wireless Communication with Dust and Sand Storms

Zainab Sh. Hammed[1,2*], Siddeeq Y. Ameen[1], and Subhi R. M. Zeebaree[1]
[1] Department of Energy Engineering, Technical College of Engineering, Duhok Polytechnic University, Duhok, Kurdistan Region, Iraq
[2] Department of Electrical and Computer, College of Engineering, University of Duhok, Kurdistan Region, Iraq
Email: Siddeeq.ameen@dpu.edu.krd, subhi.rafeeq@dpu.edu.krd

Abstract —The demands for higher throughput, data rate, low latency, and capacity in 5G communication systems prompt the use of millimeter-wave frequencies that range from 3–300 GHz with spatial multiplexing and beamforming. To get the maximum benefit from this technology, it's important to study all the challenges of using mm-wave for 5G and beyond. One of the most important impacts is weather conditions such as humidity, temperature, dust, and sand storms. This study investigates the parameters of the channel model and its statistical behavior with the effect of dust and sand storms. The latter effects can be considered the main challenges these days, especially in middle-eastern countries. A 128 x 128 massive MIMO with URA (uniformly spaced rectangular antenna arrays) uniformly spaced has been considered in the simulation assessment with mm-wave channels operating at 28 GHz and 73GHz are examined by using NYUSIM (New York University Wireless Simulator) software. The simulation results show that the dust increases the attenuation and the path loss when working at higher frequencies compared to the clear weather conditions. Moreover, their effect can be reduced by adapting the transmitted power.

Index Terms—5G, mm-Wave, NYUSIM, Massive-MIMO and channel modeling, dust and sand storm.

I. Introduction

The high-capacity applications in 5G cellular communications have pushed the amount of mobile data to new heights [1]. To support these high-capacity applications, the mm-Wave band (between 10 and 300 GHz) has been designated for 5G and beyond [2]. The other important feature of the 5G and beyond communication systems is the use of a large number of tiny cells that employ mm-wave frequencies that enhance the transmission data rate. The use of massive Multiple-Input Multiple-Output (MIMO) systems has gotten a lot of attention because they can make the spectrum much more efficient, which is needed to meet the needs of 5G and beyond [3].

The massive amount of spectrum assigned is an interesting response to the expanding bandwidth demand. There is little attenuation loss when using the 28-73GHz frequency bands for outdoor communications, and a practical mm-Wave cell radius of 200m is achieved [4], [5]. However, climate conditions significantly impact the attenuation of mobile signals due to the absorption and dispersion that can affect signal energy, which negatively influences overall system performance [6], [7].

In recent decades,dust storms have become more common in Middle Eastern countries such as Iraq, Kuwait, and Saudi Arabia. Arid regions of the world include Texas, California, and Arizona, as well as areas of arid Australia. Dust storms form when two conditions exist: first, high-speed wind, and second, the soil is dry and disjointed without any vegetation cover. The following is a mechanistic explanation of how a dust storm forms: When convection currents are produced due to heating of the earth's surface, the air above the surface warms up, causing it to rise as convection currents. This results in changes in atmospheric pressure and temperature, which then force relatively cold winds to take the place of the convection currents that were previously present. Because of this, dust rises, carrying soil grains to a level that depends on how strong the wind is, how dry the soil is, and how much it breaks apart [8].

The size of the particles distinguishes the terms dust storm and sandstorm. A dust storm happens when the particles are smaller than 0.6 mm in diameter, while a sandstorm occurs when the particles are larger than 0.6 mm in diameter (in the range of 0.6-1 mm). In addition, there are four distinct categories of dust storms [9]. The observable range is the horizontal path where the transmission reduces to two percent of its original value. It is possible to distinguish between four different types of dust storms based on how far away they are from the observation location: (i) a severe dust storm (visible range 500 meters), (ii) a moderate dust storm (visible range 0.5 to 1 kilometer), (iii) a light dust storm caused by wind (visible range 1 to 10 kilometers), and (iv) dust haze (visible range > 10 kilometers) [9]. For example, in accordance with [10], the entire country of Iraq was practically covered in a thick layer of dust after a major storm hit the country on May 16, 2022. This storm lasted for several hours, and visibility was reduced to just a few meters.

For mm-wave wireless communication networks that work at frequencies between 28 and 73 GHz, a thorough study is needed to figure out the length of coverage, the amount of path loss, and how to set up the systems. Thus,

Manuscript received August 1, 2022; revised December 14, 2022; accepted January 2, 2023.
*Corresponding author email: zainab.shawqi@dpu.edu.krd

this study aims to demonstrate the effect that dusty environments have on wireless communication channels, with a particular focus on those that operate in the 5G frequency band. This study aims to model the impacts of signal path loss, Power Delay Profile, and angular spectrum on signals sent to and received from a location. As a result, to calculate the accurate attenuation factor for any given area, it is essential to accurately measure the dielectric constant, particle size range, and dusty area concentration. In this paper, this simulation of the channel model takes into account dusty conditions, high-temperature conditions, and humidity ranges of 0%, 50%, and 100% to determine how these environmental factors influence the following parameters: path loss, received power, direction, and omnidirectional Power Delay Profile (PDP), angle of arrival, and angle of departure. An urban macrocell scenario will be suggested for the simulation, which considers the effects of dry weather.

All the previous work investigated the effect of a dust and sand storm on a single TX/RX antenna. Thus this research main contribution is to study the effect of dust and sand storm on mm-wave massive MIMO with 128 × 128 antennas. This investigation is conducted with real data particles of dust and sand storm in an urban scenario. The motivation for such investigation is versy essential because of the increased dust and sand storms recently in the middeleast countries because of climate change and the adoption of 5G and beyond.

The rest of the paper arranged such that Section II gives information on 5G massive MIMO with operating in the mm-wave band. The literature survey is addressed in Section III. Section IV discusses many varieties of approaches to modeling mm-Wave channels, as well as simulators that have been used over the years. In Section V, the impact of dust and sand storms on 5G mm-wave propagation was explored. In the last part, section VI, the results of the simulation and an explanation of those results are given. While the conclusions are discussed in section VII.

II. 5G With Massive MIMO Communication System

In recent years, a variety of novel technologies have been proposed and investigated with the goal of making 5G and beyond networks a practical reality. Several major enabling technologies for 5G and 6G systems have been suggested, including mm-waves, microcells, beamforming, device-centric design, full-duplex technology, MIMO, and massive MIMO. Mm-waves are one of the most essential enabling technologies for 5G and 6G systems. Using spatial multiplexing and MIMO antenna technology, for example, it is possible to transmit numerous concurrent streams of data over the same time and frequency resources, which is an ideal fit for MIMO technology and mobile users. High-speed data is required for a 5G network, and this will aid in the achievement of these objectives. Since the tight spacing between antenna components causes changes in the generated currents and input impedance, as well as radiation patterns, this results in a significant reduction in MIMO system capacity. Therefore, mutual coupling minimization is critical. It is as simple as separating the radiating components by a distance greater than l/2 in order to reduce correlation [11]. MIMO antennas may benefit from the usage of decoupling networks, split-ring resonators, electromagnetic bandgap structures, and faulty ground structures, all of which can be employed to reduce mutual coupling. More information on the development and manufacturing of this mutual connection for improving 5G performance can be found elsewhere[12].

Massive MIMO improves spectrum efficiency by simultaneously serving tens of terminals at the same time. As a consequence of its capacity to concentrate energy with high precision in tiny portions of space, it contributes to the improvement of overall energy efficiency. As a consequence, fading is no longer necessary and the law of large numbers and beamforming are utilized to minimize latency in its place. As a consequence of this decrease in complexity, channel hardening and frequency-domain scheduling are also lost. The whole frequency band of each resource block may be allocated to a single user using OFDM since all subcarriers have the same gain over the entire spectrum [13].

Massive MIMO employs high antenna array gain to compensate for the significant path loss experienced by mm-Wave transmissions. Mm-Wave massive MIMO systems may also benefit from the use of analog beamforming to make their implementation more straightforward. Because of its capacity, energy efficiency, and reliability, massive MIMO is an important physical layer technology for 5G communication networks. It is currently part of the 5G specification [14].

III. Literature Review

To keep pace with the increase in mobile data traffic, fundamental changes in wireless communication technologies and network architecture are needed. The 5G network was created to highly improve network speeds, latency, capacity, and energy consumption by emerging new spectrum bands, such as frequencies in the mm-Wave frequency range[15]-[17].

A large number of previous researches have addressed the characterization of channels in the mm-Wave frequency bands [19]. Different scenarios have been studied, Juneja *et al.* [18] determined outdoor access scenarios employing propagation data at frequencies of 28, 38, 60, and 73 GHz. To increase the system rate, beamforming and multi-user MIMO at mm-Wave frequencies were investigated by A. Singh *et al.* [19]. Many mm-Wave networks were layered on top of one another to produce larger macrocells, which was proposed by Mariam, *et al.* [20]. This model system architecture is used in the current 5G specifications.

Özkoç *et al*. [21] conducted an analysis and modeling of Urban Microcellular (UMi) channels operating at 28 GHz and 60 GHz.

As seen in Fig. 1, utilizing the frequency bands of 28 and 73 GHz, which are used for outdoor communications, the 77, 140, and 240 GHz bands (green circles), which only suffer 1 dB or less additional loss than caused by free space propagation per km in air [22], are suitable for longer-range broadband mobile and fixed applications. At 60 GHz, there is a "notch" in the absorption loss of about 30 GHz. According to the research, on average, attenuation loss of targeted bands is less than 0.1 dB in the 200-meter range, but at 60 GHz, it is much more (4 dB/200 m) [23].

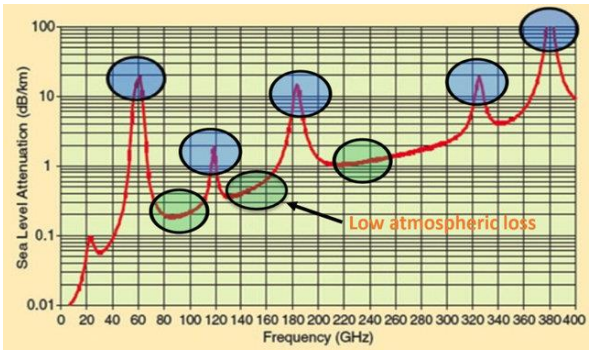

Fig. 1. The relationship between air attenuation at sea level and frequency[22].

The impact of climate weather on 5G system signals has also been considered by Shamsan [9]. He presented the results of modeling research on how storms and diffraction affect the performance of point-to-point (PPT) wireless communication links in Riyadh, Saudia Arabia. The results showed dust storms lead to an increase in free space loss at higher frequencies. The research was carried out at frequencies of 14 and 22 GHz. While Z. A. Shamsan *et al*. [24] evaluate only the effect of a dust storm, with no consideration of diffraction or atmospheric absorption losses. In [25], a modification of the Mie model has been presented to simulate the effect of a particle dust storm and investigate its attenuation based on the propagating mm-wave. At the same time, the influence of diffraction and precipitation phenomena on wireless (PPT) communication systems was investigated. In [26],the results declared that the rain attenuation was more significant, and the diffraction loss was increased at higher frequency bands.

IV. Dust and Sand Storms Effect

In order to operate at mm-wave frequencies, atmospheric phenomena such as oxygen absorption, dust, water vapor absorption, fog, and precipitation must be considered. Due to the shorter wavelength of millimeter waves, they are more prone to path loss, depolarization, and multipath effects than other types of electromagnetic waves. Attenuation is defined as the degradation of an mm-wave when it propagates through a dusty area due to variations in transmitting characteristics such as frequency, visibility, wavelength, and permittivity. Most of the dust and sand on earth comes from deserts [8].

The largest desert in Iraq covers approximately 200,000 square miles, while deserts occupy 529,000 square miles throughout Australia's whole continent [27]. The Sahara Desert, located in Northern Africa, is the largest in the world. Sand covers approximately a quarter of the world's deserts [8]. As previously indicated, the attenuation is determined by the parameters specified; a frequency that is measured in hertz is defined as the amount of time a wave passes a specified place in a given amount of time (Hz). But humidity refers to the amount of moisture in the air. The data showed that the humidity ranged from 0% (dry weather) to 100% (highly humid conditions). Another important consideration is the height (h), which is the vertical distance between the antenna and the ground. A person's visibility decreases when there is a lot of dust and sand around. Dust particles are typically between 1 and 100 μm in size, while sand particles are between 0.0625 and 2 mm [8]. The visibility is represented by Eq. (1).

$$V = \frac{0.00055}{N\, a_e^2} \tag{1}$$

where N is the number of dust particles contained within one cubic meter of air, and the unit of measurement is particles per cubic meter. Another significant measure for determining the impact of dust and sand is the dielectric constant. The moisture content of the sand defines the dielectric constant. The dielectric constant is affected by sand and dust, and it fluctuates as the moisture content of the dust/sand varies. The dielectric constant varies in response to changes in the permittivity of the sand or dust [8]. The free-space permittivity with sand and dust can be expressed as:

$$\varepsilon = \varepsilon' + j\varepsilon'' \tag{2}$$

where $\varepsilon'$is the value of the dielectric constant, and ε'' is a factor that measures the dielectric loss. As a result, Iraq is one of the arid areas prone to dust and sand storms, and the main purpose of this research is to show how dust and sand affect the operation of these mm-wave links. The radio path loss is a well-known parameter for estimating the radio coverage signal. In other words, the channel path loss determines the received signal strength. Under normal conditions, Eq. (3) determines the maximum distance between the transmitter and receiver for an optimal line of sight.

$$path\ loss_{(dB)} = 20log\left[\frac{4\pi d}{\lambda}\right] \tag{3}$$

where d is the distance in meters between two points, and λ is the wavelength in meters. It is necessary to incorporate the dusty and sand influence into the channel path loss in the event of dust and sand. The wave attenuation in free space with dust and sand can be

calculated using five different methods. These five algorithms all provide similar signal attenuation results, especially when the frequency exceeds 30GHz and the visibility is less than 20 meters [8]. The attenuation of a wave depends on several variables, but the particle radius and the distribution of the particle size are two particularly important ones. Because it considers the mutual contact phenomenon, the Mie approach is used to explore the impact of sand and dust in this paper. Visibility, height, particle size, humidity, dielectric constant, and frequency are all parameters taken into account in this method to determine attenuation. Each of these components has its own equation, however, the Mie approach combines them into a single equation that is used to compute attenuation [28]. The attenuation of dust and sand is defined as:

$$A_d = \frac{a_e f}{v}[K_1 + K_2 a_e^2 f^2 + K_3 a_e^3 f^3] \quad \frac{dB}{Km} \qquad (4)$$

where a_e is the particle's radius in meters, v is visibility in kilometers, and f is frequency operating in gigahertz (GHz).

$$K_1 = \frac{6\varepsilon_2}{(\varepsilon_1+2)^2+\varepsilon_2^2} \qquad (5)$$

$$K_2 = \varepsilon_2 \left[\frac{6}{5}\frac{7\varepsilon_1^2+7\varepsilon_2^2+4\varepsilon_1-20}{[(\varepsilon_1+2)^2+\varepsilon_2^2]^2} + \frac{1}{15} + \frac{5}{3[(2\varepsilon_1+3)^2+4\varepsilon_2^2]}\right] \qquad (6)$$

$$And\ K_3 = \frac{4}{3}\left[\frac{(\varepsilon_1-1)^2(\varepsilon_1+2)+[2(\varepsilon_1-1)(\varepsilon_1+2)-9]+\varepsilon_2^4}{[(\varepsilon_1+2)+\varepsilon_2^2]^2}\right] \qquad (7)$$

Dust and sand attenuation can be expressed as:

$$\alpha_{(dB)} = \int_0^d A_d\, dl \qquad (8)$$

The free-space path loss due to dust and sand is calculated using the proposed model, which can be written as:

$$path\ loss_{(dB)} = 20log\left[\frac{4\pi d}{\lambda}\right] + \alpha \qquad (9)$$

The mm-wave channel's free space path loss is represented in Eq. (9). Frequency, distance, dust, and sand all affect path loss, which increases as vision declines. In addition, when the radius of a specific increases, the path loss increases.

$$path\ loss_{(dB)} = 92.44 + 20log(f) + 20\,log(d) + \alpha \qquad (10)$$

where α is Dust and sand attenuation is measured in decibels (*dB*), f is the frequency operating in GHz, and d is the distance in kilometers between the transmitter and receiver. If visibility is high in typical weather circumstances, the value α is found to be small.

V. Channel Modelling

Channel modelling plays a very important role in determining the possibility of deploying the wireless communication system. Moreover, methods of channel modelling are utilized in the evaluation of both existing systems and new solutions. Thus, it is very important to investigate the most reliable channel modelling to validate any performance improvement in the 5G communication system. Various modelling techniques are applied in the evaluation of interference. Typically, they are based on an energetic evaluation of the signals that were received. However, interference level analysis might consider various factors (4, 5, 8). In order to accurately reflect the modelled problem in relation to the actual situation, it is essential to consider the important factors influencing the received signal form. The channel model and the specifications and features of antenna systems are among the first of these elements. When selecting a channel model, it is possible to take into account the environment's nature and propagation conditions, as well as the appropriate reflection of angular dispersions affecting the received signal powers. On the other hand, antenna system parameters and patterns must be taken into account. This is especially true when analyzing 5G spatial multiplexing systems, such as those that guarantee beamforming like the mMIMO system [29].

Channel modelling may be divided into two categories: deterministic and statistical. In contrast, statistical channel models are built on randomness that is considered to be inherited, with the variables being unknown. Because they do not need complicated arithmetic, calculating these models is straightforward. When statistical channel modelling is done, the path loss is used to estimate the received power of signals transmitted in a specific area. The characteristics of the channel may also be defined by statistical channel modelling using PDP and angular spectrum. Although numerous channel models have been explored in recent years, these models cannot completely characterize the behavior of the mm-wave channel. The drawback of these models is that they are insufficient to satisfy specific requirements [30].

Channel bandwidths on mmWave links will be greater than those of current systems, such as 4G because it is anticipated that they will be used for relatively high data rates. Another parameter that needs to be investigated in modelling is that both path loss and shadowing will remain rather significant obstacles in the way of reaching higher throughputs. This effect can be reduced through the use of beamforming, multi-input, multi-output systems, and highly directional antennas. For an accurate mmWave channel model, the multipath components (MPCs) must also be taken into account, and their parameters, such as amplitude, phase, and delay, must be characterized and investigated [29].

Due to the shorter wavelength of mm-Wave frequencies, MIMO antennas and beamforming techniques may help mitigate the omnidirectional path loss, which is found to be worse at frequencies than the current cellular system. The beamforming in MIMO

antennas can increase the gain of the antenna by the same size as the antenna [31]. It is possible that the path loss will be decreased as a result of the places that are not suffering outages. There is also a multipath effect, which is caused by the fact that different reflections and dispersion can cause a signal to be received more than once [32]. Spatial multiplexing could be used to take advantage of multipath effects and achieve numerous benefits [33]. Knowledge of the propagation effects of the mm-Wave channel is required to be used in the installation of wireless communication systems. When defining large-scale propagation channels, the path loss model is utilized, which explains the signal attenuation as a function of distance. Things like a lack of moisture in the air or a heavy layer of haze, as well as rain and snow, are examples of what is considered extreme weather. Using these devices may considerably improve the efficiency of a communication system, which can be quite beneficial. Massive MIMO antennas are now capable of being used in mobile and wireless communication systems, allowing them to be deployed. It is one of the MIMO systems in which the base station is equipped with several antennas [34]. It enables a large number of mobile stations to connect with the base station controller at the same time. Small-scale fading has also been decreased, resulting in faster data transfer rates and a more reliable connection. The number of antennas used at the transmitter and receiver may aid in increasing the spectral and energy efficiency of wireless communication systems [35].

The mmWave MIMO system shown in Fig. 2 is a combination of two consecutive joint segments: a digital MIMO baseband and an analog RF precoder. This system is equipped with N_T transmitters at the base station (BS) and N_R receivers at the mobile station (MS), N_S parallel data streams, and radio frequency (RF) chains, such that $N_{RF} \leq \min(N_T, N_R)$ at the transmitter and receiver. At the transmitter, N_{RF} chains are present, such that $NS < N_{RF} < N_T$ [36].

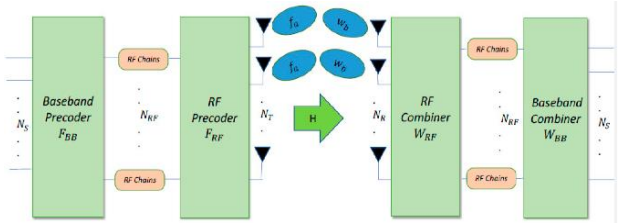

Fig. 2. Block diagram of a mmWave massive MIMO system.

A. Path Loss Model

The concept of path loss is fundamental to any wireless communication channel model and is a component of the statistical spatial channel model (SSCM) (*PL*). It helps with outage and connectivity cost calculations. The following equation considers atmospheric attenuation and the free space path loss at a reference distance of 1 m. [37]:

$$PL^{CL}(f,d)[dB] = FSPL(f,1m)[dB] + 10\,n\,log_{10}(d) + AT[dB] + X_{\sigma}^{CL} \quad (11)$$

where $d \geq 1m$, f is carrier frequency (GHz), (d) distance, attenuation term (AT), path loss exponent (PLE), and (X_{σ}^{CL}) Gaussian random variable with σ standard deviation. The path loss measured in dB at a distance of 1 m between the transmitter and receiver (T-R) is called the free space path loss (f,1m) and is given by;

$$FSPL(f,1m)[dB] = 20\ log_{10}\left(\frac{4\pi f \times 10^9}{c}\right) = 32.4[dB] + 20log_{10}(f) \quad (12)$$

where c is the speed of light in vacuum, and f is in GHz. The term AT is characterized by:

$$AT[dB] = \alpha[dB/m]\ \times d[m] \quad (13)$$

where α in dB/m is the attenuation factor in the region of 1GHz to 100GHz. This factor takes into account the combined effects of haze, water vapor, rain, and dry air attenuation [38]. In Eq. (1), the 3D T-R separation distance is referred to as the parameter d.

B. Delay Spread and Power Delay Profile

It is essential to recognize that the power delay profile (PDP) is an important factor in determining the signal's strength when received in an environment with multipath. PDP is affected by time delay since it has a shape that declines exponentially with time. The spread of delay may be used to characterize several aspects of multipath channel time dispersion. It is considered to be formed from PDP and may be disseminated across the latter due to the fact that it is a collection of multipath with high energy. Furthermore, the channel's DS is an essential metric for estimating the amount of system overhead required to enable communication [39].

Delay spread may be calculated by using the root mean square approach and using the second central instant of the power delay profile as the starting point. For the purpose of calculating delay spread, the following may be used [39]:

$$\sigma_t = \sqrt{\overline{t^2} - (\bar{t})^2} \quad (14)$$

where

$$\overline{t^2} = \frac{\sum_n p(t) t_n^2}{\sum_n P(t_n)}\ \&\ \bar{t} = \frac{\sum_n p(t)\tau_n}{\sum_n P(\tau_n)} \quad (15)$$

The parameter $\bar{t}$, is the excess mean delay; it is the first central moment and $\overline{t^2}$ is the power delay profile's second central moment. P(t_n) is the milliwatt power of the delay bin that corresponds to the delay bin t_n.

VI. Simulation Results and Assessment

The results of this research were obtained by employing frequency bands at 28 GHz and 73.5 GHz,

respectively, to evaluate the behavior of the channel in an urban macrocell with an 800 MHz bandwidth. Although the channel number in the Uma (urban macrocell) scenario is more than that in the Umi (urban microcell) channel, Umi is more variable for various frequency components than the Uma channel. This is because the power delay profile generated in the Umi scenario has a more significant gain than the profile developed in the Uma scenario. Consequently, the channel in the Umi circumstance is more warped than in the Uma circumstance. So, the Uma situation has resulted in an improvement in SER efficiency. When channel simulations are performed, meteorological factors like dust storms, sand, humidity, temperature, and vegetation are present. The channel model simulator for NYUSIM, which works between 2 GHz and 100 GHz, was employed to produce these simulation results. NYUSIM software, an open-source channel simulator, is used in this study to propose a model for massive MIMO at 28–73 GHz [40]. The channel and antenna parameters, on the other hand, are listed in Table I and Table II.

TABLE I: CHANNEL PARAMETER

Parameters	values
Frequency	28 GHz and 73 GHz
RF Bandwidth	800 MHz
Scenario	Uma
Environment	LOS
Lower Bound of T-R distance	10 m
Upper Bound of T-R distance	100 m
Tx-Power	30 dBm
Barometric Pressure	1013.25 mbar
Humidity	0,50,and 100 %
Temperature	45 o C
Rain Rate	0 mm/hr
Polarization	Co-Pol
Foliage	0.4 dB/m
Transmitting Array type	Uniform Rectangular Array
Receiving Array type	Uniform Rectangular Array
Dielectric constant	$\varepsilon' = 4.56, 3.50,$ $\varepsilon'' = 0.25, 1.64$

TABLE II: ANTENNA PARAMETERS

Antenna Parameters	values
Number of Tx antenna	128
Number of Rx antenna	128
Tx antenna azimuth HPBW	10º
Tx antenna elevation HPBW	10º
Rx antenna azimuth HPBW	10º
Rx antenna elevation HPBW	10º
Tx Antenna Spacing	0.5 λ
Rx Antenna Spacing	0.5 λ

TABLE III: DUST STORM ATTENUATION AND PATH LOSS EFFECT

Case	a_e (μm)	V(Km)	Ad (dB/ Km)		Path Loss	
			28GHz	73GHz	28GHz	73GHz
1	20	0.6	1.0211	7.431	119.4	146.3
2	14	1	0.4289	3.291	116.4	125.6
3	8	2	0.1225	1.0234	114.8	114.2
4	3	4	0.0230	0.4331	114.4	111.3

The results in Table III and Table IV show that the attenuation is related to frequency but inversely proportional to the visibility of a dust storm. As a result, one of the conclusions that could be reached is that as the severity of the dust storm increases, so does the signal attenuation. Another obvious conclusion is that signal attenuation rises in proportion to the incident electromagnetic wave frequency. Additionally, the received power decreased from -66.5 dBm to -79.7 dBm and from -76 dBm to -78.81dBm for 28GHz and 73GHz, respectively, as shown in Figs. 3–6. When frequency, dielectric constants, and visibility are all taken into account, it was also found that the calculated attenuation is the same as what can be found with existing models.

TABLE IV: SAND STORM ATTENUATION AND PATH LOSS

Case	a_e (mm)	V(Km)	Ad (dB/ Km)		Path Loss	
			28GHz	73GHz	28GHz	73GHz
1	2	0.00005	4.58	12.03	118.68	123.23
2	1	0.0002	1.35	3.57	115.45	114.77
3	0.1	0.02	0.989	1.0234	115.09	112.22
4	0.06	0.065	0.0342	0.0632	114.23	111.26

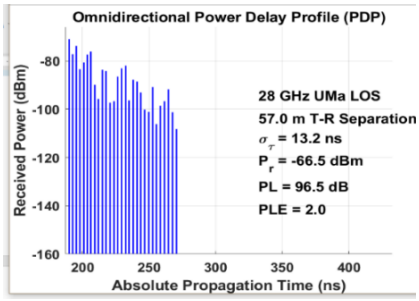

Fig. 3. Omnidirectional- PDP at 28 GHz without the effect of dust and sand.

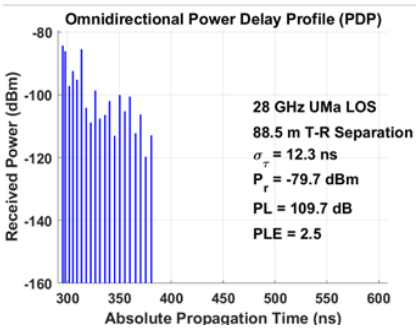

Fig. 4. Omnidirectional- PDP at 28 GHz with the effect of dust and sand.

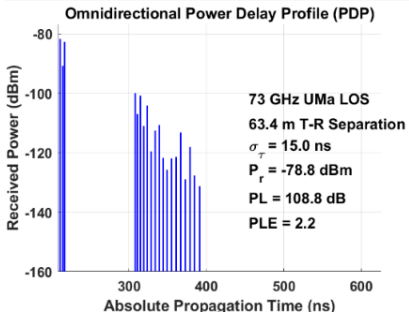

Fig. 5. Omnidirectional- PDP at 73GHz without the effect of dust and sand.

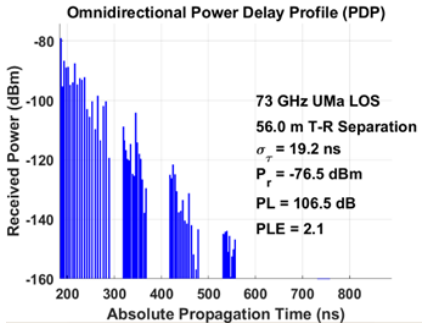

Fig. 6. Omnidirectional- PDP at 73 GHz with the effect of dust and sand.

The filtering of many Multipath Components (MPCs) by a directional antenna is more complicated than filtering them by an omnidirectional antenna.This results in a higher directional path loss after subtracting the antenna gain from the received power [37].

Fig. 7 and Fig. 8 illustrate the results of the PDP simulation for the omnidirectional antenna at 28 and 73 GHz, respectively. Because no blocking materials interfere with the signal power as it travels from the T_x to the R_x and the environment has little impact on the signal power, many components arrive at the R_x with a high magnitude in the case of the LOS environment.

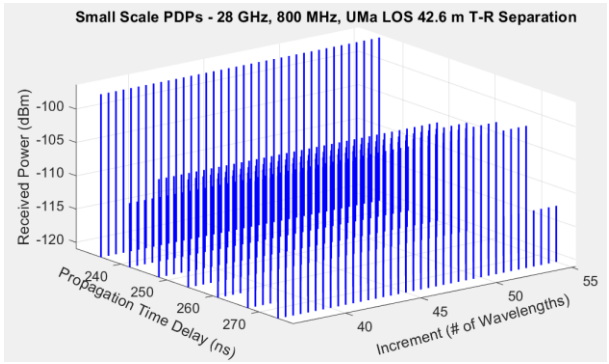

Fig. 7. Small-Scale PDP at 28 GHz.

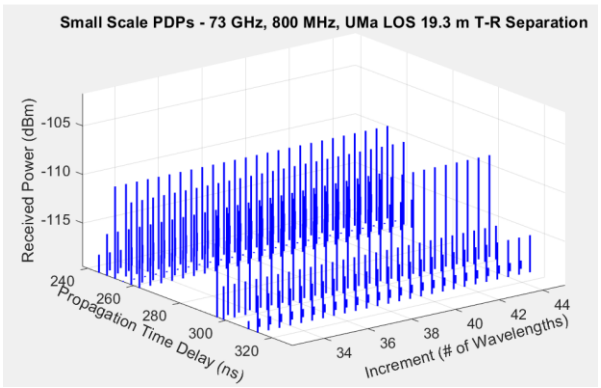

Fig. 8. Small-Scale PDP at 73 GHz.

The path losses obtained for the 28-GHz and 73-GHz frequency bands are shown in Fig. 9 and Fig. 10, respectively. When producing this data, the Tx and Rx antenna azimuth and elevation HPBWs are set to 10° for LOS antenna azimuth and height HPBWs. The data displayed below was obtained via the use of 100 simulations, each of which covered a distance ranging between 50 meters and 500 meters. Apart from PLE and "σomni," it's also worth noting that "dir." stands for direction, "σdir-best" represents the maximum received power, and "Omni" denotes the whole field all represented by the letter "dir."

The path loss at 73 GHz is often higher than the path loss at 28 GHz. It has been observed that there is a clear relationship between frequency and path loss. Given that path loss changes with distance, it is estimated that at a distance of 100 meters, path loss increases by about 10 dB.

Although the exponent for directional path loss in Figs. 9-12 was calculated using arbitrary unique pointing angles, the exponent for directional path loss was increased in dusty weather from 8dB to 8.5dB and from 14.3dB to 11.2 dB for 28GHz and 73GHz respectively. As a result, beamforming at the base station and the mobile device is crucial for increasing the Signal-to-Noise Ratio (SNR) and expanding coverage distances in this scenario.

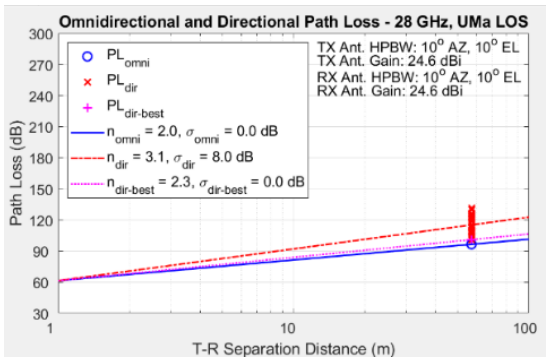

Fig. 9. PL for 28GHz band (LOS)without effect of dust and sand.

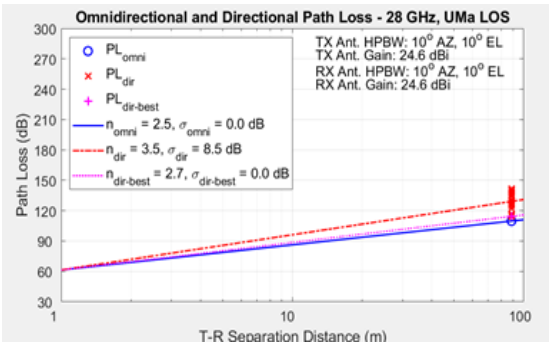

Fig. 10. PL at 28GHz band (LOS)with effect of dust and sand.

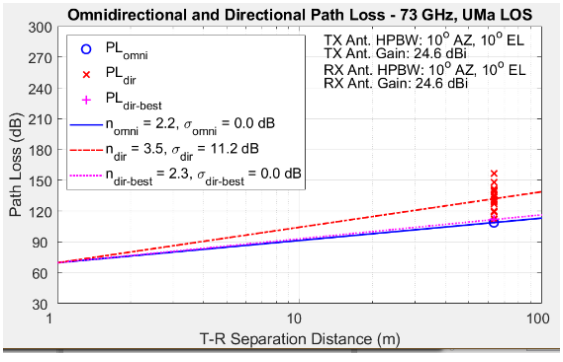

Fig. 11. PL at 73 GHz band (LOS)without the effect of dust and sand.

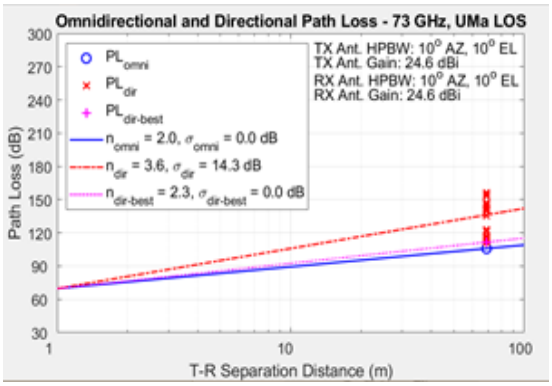

Fig. 12. PL at 73GHz band (LOS) with the effect of dust and sand.

The results presented show the performance of the Massive MIMO system for (28,73) GHz frequency bands for outdoor communication employed in 5G and 6G. The investigation showed that these high frequencies have an excellent coverage distance between 100–500 m, with a transmitting power of 30 dBm and 45 dBm at the transmitter, reasonable path loss, and short r.m.s delay spread, which leads to large coherence bandwidth. There is a slight difference in coverage distance, path loss, and other parameters between (28–73) GHz. However, both frequencies are suitable for 5G and beyond. Consequently, the results indicate that the channel model supports various scenarios such as indoor, urban, suburban, rural areas, etc.. Furthermore, the channel model shows that a reliable operation with various high-speed train scenarios, including open space, viaduct, cutting, tunnels, etc. can be achieved.

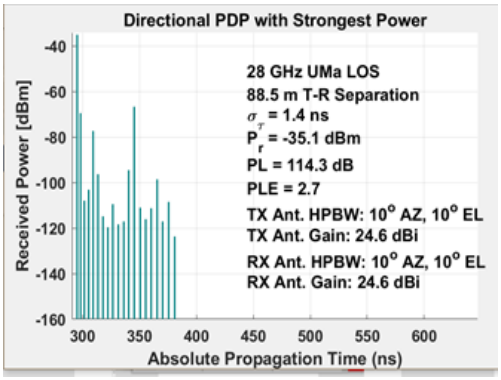

Fig. 13. Directional- PDP at 28 GHz.

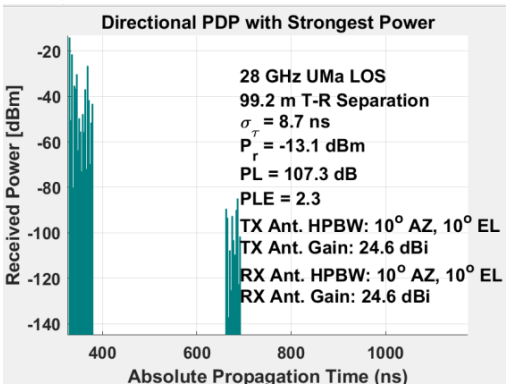

Fig. 14. Directional- PDP at 28 GHz, and Pt=45dB.

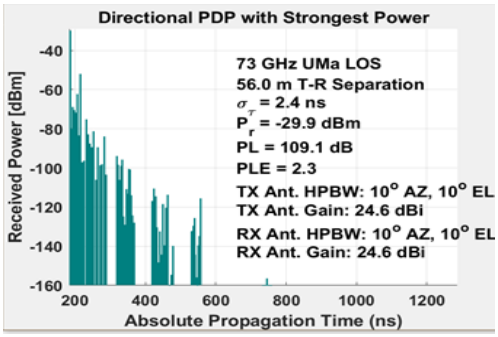

Fig. 15. Directional- PDP at 73 GHz.

To reduce the effects of dust, the transmitted power has to increase during the dust storm and sand to compensate for the attenuation. From Figs. 13–16, we can see that the received power went from -35.1 to 13.1 dBm at 28 GHz and from -29.9 to 0.5 dBm at 73 GHz. This caused the transmitted power to increase by 45 dB.

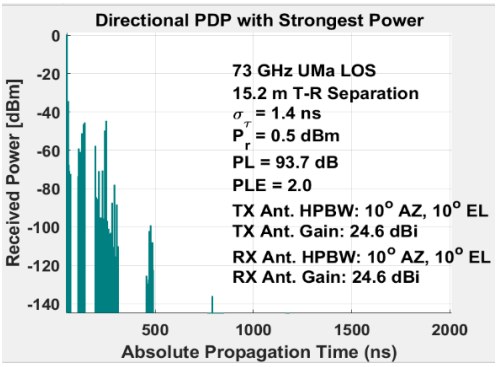

Fig. 16. Directional- PDP at 73 GHz, and Pt=45dB.

Higher frequencies have been shown to be more essential than lower frequencies in the simulations, with path loss and multipath propagation being more significant at higher frequencies. The use of mm-Wave increases the spectrum bandwidth by 10 times, which leads to better transmission speeds and low latency. Thus, increased radio spectrum frequencies result in higher losses, which impacts system performance and necessitates careful system design, particularly regarding the shortest possible distance between transmitter and receiver. Also, 5G systems need to use the best receivers possible, especially for mm-waves and other very high operating frequencies.

VII. Conclusion

The paper uses massive MIMO techniques with 5G requirements and specifications to analyze the propagation channel at 28 and 73 GHz in an urban macrocell scenario. Massive MIMO scenarios with 128 × 128 have been assumed to examine the channel characteristics within LOS environments. Simulation findings of millimeter-wave channel modelling have been conducted for urban macrocells showing the impacts of atmospheric impairments such as dust and sand storms, which have increased in the last decades in Middle

Eastern countries. Practical dust storm data has been employed to investigate its effect on channel modelling. The channel model provides a realistic channel parameter and SE prediction due to the use of extensive real-world measurement data at mm-wave frequencies.

CONFLICT OF INTEREST

The authors whose names are listed immediately below certify that they have NO affiliations with or involvement in any organization or entity with any financial interest (such as honoraria; educational grants; participation in speakers' bureaus; membership, employment, consultancies, stock ownership, or other equity interest; and expert testimony or patent-licensing arrangements), or non-financial interest (such as personal or professional relationships, affiliations, knowledge or beliefs) in the subject matter or materials discussed in this manuscript.

AUTHOR CONTRIBUTION

The authors confirm contribution to the paper as follows:

Study conception and design:

Zainab Sh. Hammed, Siddeeq Y. Ameen; data collection: Zainab Sh. Hammed; analysis and interpretation of results: Zainab Sh. Hammed, Siddeeq Y. Ameen, Subhi R. M. Zeebaree; draft manuscript preparation: Zainab Sh. Hammed, Siddeeq Y. Ameen, Subhi R. M. Zeebaree.

All authors reviewed the results and approved the final version of the manuscript.

The author confirms sole responsibility for the following: study conception and design, data collection, analysis and interpretation of results, and manuscript preparation.

1. Have made a substantial contribution to the concept or design of the article; or the acquisition, analysis, or interpretation of data for the article; AND

2. Drafted the article or revised it critically for important intellectual content; AND

3. Approved the version to be published; AND

4. Agreed to be accountable for all aspects of the work in ensuring that questions related to the accuracy or integrity of any part of the work are appropriately investigated and resolved.

REFERENCES

[1] N. Lal, S. M. Tiwari, D. Khare, and M. Saxena, "Prospects for handling 5G network security: Challenges, recommendations and future directions," *Journal of Physics: Conference Series*, vol. 1714, no. 1, p. 12052, 2021.

[2] A. Bonfante, L. G. Giordano, I. Macaluso, and N. Marchetti, "Performance of predictive indoor mmwave networks with dynamic blockers," *IEEE Trans. Cogn. Commun. Netw.*, 2021.

[3] M. Rebato, L. Rose, and M. Zorzi, "Performance assessment of MIMO precoding on realistic mmWave channels," in *Proc. IEEE International Conference on Communications Workshops, ICC Workshops*, 2019, pp. 1–6.

[4] A. Morgado, K. M. S. Huq, S. Mumtaz, and J. Rodriguez, "A survey of 5G technologies: Regulatory, standardization and industrial perspectives," *Digit. Commun. Networks*, vol. 4, no. 2, pp. 87–97, 2018.

[5] J. Sachs and K. Landernäs, "Review of 5G capabilities for smart manufacturing," in *Proc. of the International Symposium on Wireless Communication Systems*, 2021, pp. 1–6.

[6] J. Huang, Y. Cao, X. Raimundo, A. Cheema, and S. Salous, "Rain statistics investigation and rain attenuation modeling for millimeter wave short-range fixed links," *IEEE Access*, vol. 7, pp. 156110–156120, 2019.

[7] S. Zang, M. Ding, D. Smith, P. Tyler, T. Rakotoarivelo, and M. A. Kaafar, "The impact of adverse weather conditions on autonomous vehicles: How rain, snow, fog, and hail affect the performance of a self-driving car," *IEEE Veh. Technol. Mag.*, vol. 14, no. 2, pp. 103–111, 2019.

[8] E. M. M. Abuhdima, *et al*., "The effect of dust and sand on the 5G Millimeter-Wave links," in *Proc. IEEE Int. Conf. Wirel. Sp. Extrem. Environ. WiSEE* 2021, 2021, pp. 60–65.

[9] Z. A. Shamsan, "Dust storm and diffraction modelling for 5g spectrum wireless fixed links in arid regions," *IEEE Access*, vol. 7, pp. 162828–162840, 2019.

[10] F. Tajiki, H. M. Asgari, I. Zamani, and F. Ghanbari, "Assessing the relationship between airborne fungi and potential dust sources using a combined approach," *Environ. Sci. Pollut. Res.*, vol. 29, no. 12, pp. 17799–17810, 2022.

[11] Z. S. Hammed, S. Y. Ameen, and S. R. M. Zeebaree, "Massive MIMO-OFDM performance enhancement on 5G," in *Proc. 29th International Conference on Software, Telecommunications and Computer Networks, SoftCOM*, 2021, pp. 1–6.

[12] I. Nadeem and D. Y. Choi, "Study on mutual coupling reduction technique for MIMO antennas," *IEEE Access*, vol. 7, pp. 563–586, 2019.

[13] S. A. Busari, K. M. S. Huq, S. Mumtaz, L. Dai, and J. Rodriguez, "Millimeter-Wave massive MIMO communication for future wireless systems: A survey," *IEEE Commun. Surv. Tutorials*, vol. 20, no. 2, pp. 836–869, 2018.

[14] E. Bjornson, L. Van Der Perre, S. Buzzi, and E. G. Larsson, "Massive MIMO in sub-6 GHz and mmWave: Physical, practical, and use-case differences," *IEEE Wirel. Commun.*, vol. 26, no. 2, pp. 100–108, 2019.

[15] M. A. Qureshi and C. Tekin, "Online bayesian learning for rate selection in millimeter wave cognitive radio networks," in *Proc. IEEE INFOCOM*, 2020, vol. 2020-July, pp. 1449–1458.

[16] A. Ahad, M. Tahir, and K. L. A. Yau, "5G-based smart healthcare network: Architecture, taxonomy, challenges and future research directions," *IEEE Access*, vol. 7, pp. 100747–100762, 2019.

[17] A. Al-Omary, "Investigating the visibility of 28 and 73 GHz frequency bands for outdoor MIMO channel," *Int. J. Comput. Digit. Syst.*, vol. 9, no. 3, pp. 503–513, 2020.

[18] S. Juneja, R. Pratap, and R. Sharma, "Semiconductor technologies for 5G implementation at millimeter wave frequencies – Design challenges and current state of work," *Eng. Sci. Technol. An Int. J.*, vol. 24, no. 1, pp. 205–217, 2021.

[19] A. Singh and S. Joshi, "A survey on hybrid beamforming in MmWave massive MIMO system," *J. Sci. Res.*, vol. 65, no. 1, pp. 201–213, 2021.

[20] H. Mariam, I. Ahmed, and M. I. Aslam, "Coverage probability of uplink millimeter wave cellular network with non-homogeneous interferers' point process," *Phys. Commun.*, vol. 45, p. 101274, 2021.

[21] M. F. Ozkoc, A. Koutsaftis, R. Kumar, P. Liu, and S. S. Panwar, "The impact of multi-connectivity and handover constraints on millimeter wave and terahertz cellular networks," *IEEE J. Sel. Areas Commun.*, vol. 39, no. 6, pp. 1833–1853, 2021.

[22] Y. Xing and T. S. Rappaport, "Propagation measurement system and approach at 140 GHz-Moving to 6G and above 100 GHz," in *Proc. IEEE Global Communications Conference, GLOBECOM*, 2018, pp. 1–6.

[23] A. Gupta, M. Tripathi, P. L. P. Kumar, and A. V. H. Vardhan, "Analysis of 5G channel parameters using mmWave channel simulator NYUSIM," *Intell. Circuits Syst.*, pp. 351–357, 2021.

[24] Z. A. Shamsan, M. Alammar, A. Alharthy, A. Aldahmash, K. A. Al-Snaie, and A. M. Al-Hetar, "Micrometer and millimeter wave P-to-P links under dust storm effects in arid climates," *Eng. Technol. Appl. Sci. Res.*, vol. 9, no. 4, pp. 4520–4524, 2019.

[25] E. M. M. Abuhdima, *et al*., "Impact of weather conditions on 5G communication channel under connected vehicles framework," arXiv Prepr. arXiv2111.09418, 2021.

[26] Z. A. Shamsan, "Rainfall and diffraction modeling for Millimeter-Wave wireless fixed systems," *IEEE Access*, vol. 8, pp. 212961–212978, 2020.

[27] O. F. Al-Sheikhly, "A preliminary pictorial guide to the herpetofauna of tigris and euphrates river basin," in *Tigris and Euphrates Rivers: Their Environment from Headwaters to Mouth*, Springer, 2021, pp. 1007–1040.

[28] E. Abuhdima, *et al*., "Impact of dust and sand on 5G communications for connected vehicles applications," *IEEE J. Radio Freq. Identif.*, 2022.

[29] M. S. Kumari and N. Kumar, "Channel model for simultaneous backhaul and access for mmWave 5G outdoor street canyon channel," *Wirel. Networks*, vol. 26, no. 8, pp. 5997–6013, 2020.

[30] D. Pinchera, M. Migliore, and F. Schettino, "Compliance boundaries of 5G massive MIMO radio base stations: A statistical approach," *IEEE Access*, vol. 8, pp. 182787–182800, 2020.

[31] L. Kong, M. K. Khan, F. Wu, G. Chen, and P. Zeng, "Millimeter-Wave wireless communications for IoT-cloud supported autonomous vehicles: Overview, design, and challenges," *IEEE Commun. Mag.*, vol. 55, no. 1, pp. 62–68, 2017.

[32] B. Wang, F. Gao, S. Jin, H. Lin, and G. Y. Li, "Spatial-and frequency-wideband effects in Millimeter-Wave massive MIMO systems," *IEEE Trans. Signal Process.*, vol. 66, no. 13, pp. 3393–3406, 2018.

[33] N. Keshav, "Millimetre Wave communication with spatial division multiplexing for 5G systems," *Turkish J. Comput. Math. Educ.*, vol. 12, no. 7, pp. 2609–2616, 2021.

[34] M. M. Tamaddondar and N. Noori, "3D Massive MIMO channel modeling with cluster based ray tracing method," in *Proc. 27th Iranian Conference on Electrical Engineering*, 2019, pp. 1249–1253.

[35] S. Mumtaz, J. Rodriguez, and L. Dai, "mmWave Massive MIMO," 2017.

[36] P. S. Srivastav, L. Chen, and A. H. Wahla, "Precise channel estimation approach for a mmWave MIMO system," *Appl. Sci.*, vol. 10, no. 12, p. 4397, 2020.

[37] N. Ram, H. Gao, H. Qin, M. T. Oo, and Y. T. Htun, "Statistical channel modelling of millimetre waves at 28 GHz and 73 GHz frequency signals using MIMO antennas," *Journal of Physics: Conference Series*, vol. 1732, no. 1, p. 12184, 2021.

[38] S. Sun, *et al*., "Investigation of prediction accuracy, sensitivity, and parameter stability of large-scale propagation path loss models for 5G wireless communications," *IEEE Trans. Veh. Technol.*, vol. 65, no. 5, pp. 2843–2860, 2016.

[39] S. Sun, G. R. Maccartney, and T. S. Rappaport, "A novel Millimeter-Wave channel simulator and applications for 5G wireless communications," in *Proc. IEEE International Conference on Communications*, 2017, pp. 1–7.

[40] R. Játiva, A. Salazar, and W. Toscano, "Reference models for 5G wireless communications channels," in *Proc. IEEE Fourth Ecuador Technical Chapters Meeting*, 2019, pp. 1–6.

Zainab Sh. Hammed was born in Baghdad, Iraq, in 1980. She got the BSc. and MSc. degree from University of Technology-Baghdad-Iraq at 2002, and 2009 respectively, both in communication engineering. She is currently pursuing the Ph.D. degree with the Department of Electrical and Computer Engineering, Duhok University. Her research interests include wireless communication, channel estimation,5G system and beyond.

Siddeeq Y. Ameen received BSc in Electrical and Electronics Engineering in 1983 from University of Technology, Baghdad. Next, he was awarded the MSc and Ph.D. degree from Loughborough University, UK, respectively in 1986 and 1990 in the field of Digital Communication Systems and Data Communication. From 1990- 2006, Professor Siddeeq worked with the University of Technology in Baghdad with participation in most of Baghdad's universities. From Feb. 2006 to Sep. 2011 he was a Dean of Engineering College at the Gulf University in Bahrain. From Oct. 2011-Sep. 2015 he joined the University of Mosul, College of Electronic Engineering as a Professor of Data Communication and next Dean of Research and Graduate Studies at Applied Science University, Bahrain till Sep. 2017. Presently, he is a research centrer director at Duhok Polytechnic University, Duhok, Iraq. Through his academic life, he published over 130 papers and a patent in the field of data communication, computer networking and information security and supervised over 120 Ph.D. and MSc research students. He won the first and second best research in Information Security by the Arab Universities Association in 2003.

Subhi R. M. Zeebaree was born in Duhok, Iraq, in 1968. He got his BSc, MSc and Ph.D. Degrees from University of Technology-Baghdad-Iraq at 1990, 1995 and 2006 respectively. both in communication engineering. She is currently pursuing the Ph.D. degree with the Department of Electrical and Computer Engineering, Duhok University. He is a member of the IEEE Iraq section. He participated in more than fifteen international IEEE conferences. He has more than 150 papers and books published by (Clarivate, SCOPUS, DOAJ, and DOI) indexed journals and conferences.